Science of Sintering, **48** (2016) 333-341

doi: 10.2298/SOS1603333E

UDK 535.375; 543.4

The Bridgman Method Growth and Spectroscopic Characterization of Calcium Fluoride Single Crystals

Hana Ibrahim Elswie[1, 2], Zorica Ž. Lazarević[3*)], Vesna Radojević[1], Martina Gilić[3], Maja Rabasović[3], Dragutin Šević[3], Nebojša Ž. Romčević[3]

[1]Faculty of Technology and Metallurgy, University of Belgrade, Belgrade, Serbia
[2]Faculty of Science, Department of Science, Tripoli University, Tripoli, Libya
[3]Institute of Physics, University of Belgrade, Pregrevica 118, Zemun, Belgrade, Serbia

Abstract:

It must be noted that the main objective of this study was to obtain single crystals of calcium fluoride - CaF_2, and after that the crystals were characterized with various spectroscopic methods. The crystals were grown using the Bridgman technique. By optimizing growth conditions, <111> oriented CaF_2 crystals up to 20 mm in diameter were grown. Number of dislocations in CaF_2 crystals was 5×10^4 - 2×10^5 per cm^2. Selected CaF_2 single crystal is cut into several tiles with the diamond saw. The plates were polished, first with the silicon carbide, then the paraffin oil, and finally with a diamond paste. The obtained crystal was studied by Raman and infrared -IR spectroscopy. The crystal structure is confirmed by X-ray diffraction (XRD). One Raman and two IR optical modes predicted by group theory are observed. A low photoluminescence testifies that the concentration of oxygen defects within the host CaF_2 is small. All performed investigations show that the obtained CaF_2 single crystal has good optical quality, which was the goal of this work.

Keywords: *CaF_2, Raman spectroscopy, IR spectroscopy, Photoluminescence.*

1. Introduction

Single crystals, especially calcium fluoride (CaF_2) single crystals, are required as starting materials for optical components in DUV-photolithography, such as steppers or excimer lasers. They are conventionally used as lenses or prisms [1, 2]. They are especially used to optically copy fine structures into integrated circuits, computer chips and/or photo-lacquer-coated wafers [3, 4]. Crystals, in principle, can be grown from the gas phase, the melt, from solution and even from a solid phase by recrystallization or solid body diffusion [5]. Different processes for crystal growth are described in text books for crystal growth, such as the 1088 page work of Wilke and Bohm [6].

For excellent optical quality, intense studies have been undertaken on each stage of producing CaF_2 crystal, from raw materials purification [7, 8], growth parameters optimization [9], growth technique innovation [10-12], annealing [13] and surface machining improvement [14]. Among these stages, crystal growth technique is the most radical and crucial. The main techniques for CaF_2 single crystal growth are the Czochralski [15], Bridgman-Stockbarger [11], and gradient solidification methods [10], which all possess

*) **Corresponding author:** lzorica@yahoo.com

respective advantages and drawbacks. It seems significant to find a more effective method for high-quality and large-dimension CaF_2 crystals. However single crystals for industrial applications are usually grown by solidification from a melt [16]. The so-called Stockbarger-Bridgeman and the vertical gradient freeze processes are used for industrial manufacture of single crystals [17]. The crystals are grown in a drawing oven and in a vacuum of 10^{-4} to 10^{-5} mbar in the Stockbarger-Bridgeman method. A crystalline raw material is melted, so that a homogeneous single crystal is obtained with exacting control of temperature. CaF_2 single crystals of more than 10 inches in diameter are required for the lens materials. Such large CaF_2 single crystals are grown by the Czochralski method [18, 19] or the vertical Bridgman method [20, 21].

CaF_2 is an ionic crystal with the fluorite structure [22]. Unit cell of CaF_2 is presented in Fig. 1. The crystal lattice is a face centered cubic (fcc) structure with three sublattices. The fluorite structure, seen in calcium fluoride, has the calcium ions in a face centered cubic array with the fluoride ions in all (8) of the tetrahedral holes. The fluoride ions have a coordination number 4, and the calcium ions have a coordination number 8. The natural cleavage plane of the crystal is the <111> surface. In Fig. 1, the four possible <111> planes are defined by F^--ion Ca^{2+}-ion a respective triple of the four Ca^{2+} ions [23]. The melting point of CaF_2 is at 1347 °C. At a temperature of 1147 °C, a maximum of the specific heat is observed that is caused by melting of the fluorine sublattice. The fluorine ions are randomly distributed over the normal lattice sites (tetrahedral coordinated) and the interstitial sites (octahedral coordinated). The ionic mobility consequently becomes very high. The behavior is known as superionic conduction, it is observed in a variety of materials with the fluorite structure [24].

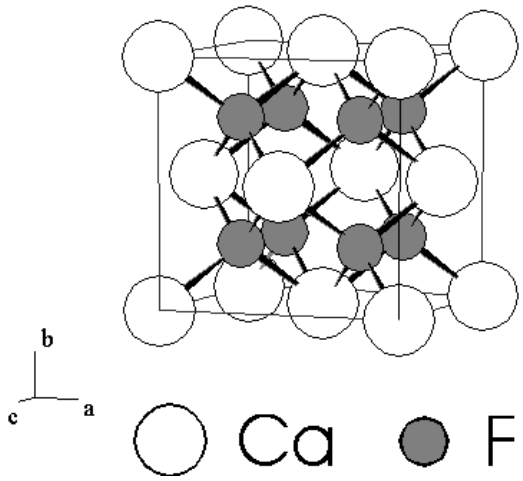

Fig. 1. Unit cell representation of CaF_2 structure.

Single crystal CaF_2 used in the optical devices can be of natural origin - fluorite, under which name is often referred to in literature [25], and synthetic single crystal CaF_2 which is usually obtained by the growth from the melt. CaF_2 requires the use of special growth conditions to obtain quality crystals because of its specific chemical and physical properties: relatively high melting point (over 1300 °C), high chemical aggressiveness of fluorine at these temperatures, relatively small chemical stability at high temperatures and very strong ability to react with traces of water vapor. Therefore, the growth of a single crystal CaF_2 may take place either in vacuum or in an inert gas atmosphere (argon or helium) at purity of at least 99.99% in order to prevent the presence of traces of moisture or oxygen.

It may be noted that the Bridgman method is one of the most popular methods of crystal growth because it is very easy to perform in a vacuum and in an inert atmosphere [26, 27]. The method consists in the fact that the rate of the entire batch of CaF_2 in the crucible, which is of cylindrical shape with a conical bottom, and then is lowered into the crucible

colder part of the furnace, so that the crystallization process begins at the bottom of the crucible at the top of the cone. Reviewing the literature it can be noted that the crucible can be made from spectroscopically pure graphite [20, 21, 25, 28, 29] or platinum [30].

The aim of our work was to produce CaF_2 single crystal of good optical quality. The structural and optical properties obtained crystals were characterized using Raman, IR and luminescence spectroscopy.

2. Experimental procedure

The BCG365 device was used to obtain single crystals of CaF_2 by Bridgman method. Initial samples of single crystals were mostly transparent, but some were cracked. Therefore, we had to make some changes in conditions of growth and construction of crucible. Experiments have been performed with CaF_2 in the form of a powder. The CaF_2 powder was compacted and sintered in the form of tablets. Crucible could easily be filled with such obtained tablets. Powder CaF_2 (Rare Earth Products Limited) purity of 99.99% was used in the experiment. It was compacted under a pressure of 3500 kg cm^{-2}, and the sintering of the obtained tablets was carried out at 900 °C under an inert atmosphere of argon. We tried out combinations of various growth rates and generator powers with the aim to define the optimal growth conditions. Power generator was initially P_{gen} = 3.8 kW, and was later increased to P_{gen} = 3.94 kW. The crystal growth rates were 6 mm h^{-1}, 12 mm h^{-1}, 24 mm h^{-1}, and 48 mm h^{-1}.

The observations relating to the dislocation were recorded by observing an etched surface of CaF_2 crystal, using a Metaval of Carl Zeiss Java metallographic microscope with magnification of 270x. A selected CaF_2 single crystal was cut into several tiles with the diamond saw. The plates were polished, first with the silicon carbide, then the paraffin oil, and finally with a diamond paste. The obtained finely polished sample, which were later used for the characterization of Raman, IR and luminescence spectroscopy. The crystal plane of cleavage of calcium fluoride crystal is <111>. Thin panels for testing dislocations we obtained by splitting of individual pieces of crystal. Conc. H_2SO_4 is used as an etching solution, gave a sample that was etched for 15 min.

The Raman scattering measurements of CaF_2 crystal was performed in the backscattering geometry at room temperature in the air using a Jobin-Yvon T64000 triple spectrometer, equipped with a confocal microscope (100x) and a nitrogen-cooled charge coupled device detector (CCD). The spectra have been excited by a 514.5 nm line of Coherent Innova 99 Ar^+ - ion laser with an output power of less than 20 mW to avoid local heating due to laser irradiation. Spectra were recorded in the range from 100 to 800 cm^{-1}.

The room temperature far- infrared reflectivity measurements was carried out with a BOMEM DA-8 FIR spectrometer. A DTGS pyroelectric detector was used to cover the wave number range from 50 to 600 cm^{-1}.

Photoluminescence (PL) studies reported in this work were performed at room temperature using Optical Parametric Oscillator (Vibrant OPO) tuned at 350 nm as excitation source. Time resolved streak images of the emission spectrum excited by OPO system are collected by using a spectrograph (SpectraPro 2300i) and recorded with a Hamamatsu streak camera (model C4334). All streak camera operations are controlled by the HPD-TA (High Performance Digital Temporal Analyzer) software.

3. Results and discussions

CaF_2 single crystals are obtained by the vertical Bridgman method in vacuum. The best results were obtained with a crystal growth rate of 6.8 mm h^{-1}. The obtained single crystal of CaF_2 was 90 mm in length and 20 mm in diameter (Fig. 2).

Fig. 2. Photographs of Bridgman-grown CaF_2 single crystal.

The general conclusion is that in all samples relatively high dislocation density was observed (ranging from 60000 to 140000) as a consequence of greater internal stresses, which have emerged in the process of cooling. From the Fig. 3, the dislocations of CaF_2 can be observed. Etch pits have the shape of a three-sided pyramid. Number of dislocations in CaF_2 crystals which were made by the method of Bridgman was $5x10^4$ - $2x10^5$ per cm^2.

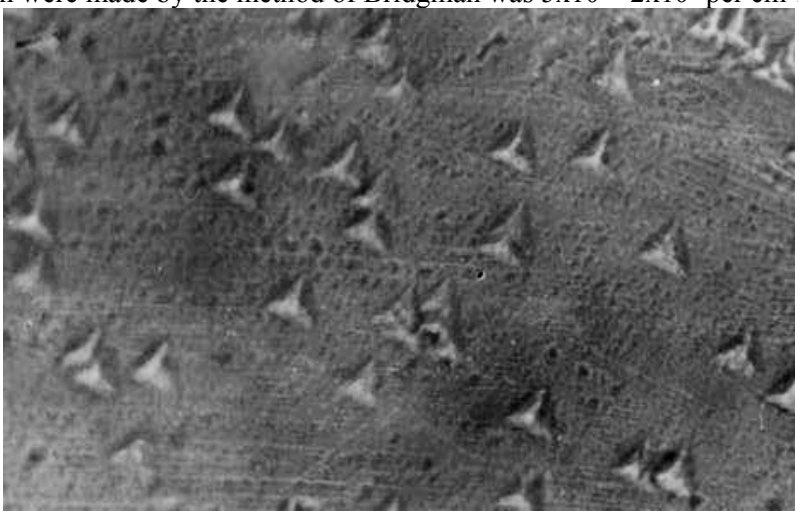

Fig. 3. The microscopic image of the surface CaF_2 crystal plate in the direction <111>. Magnification of 270x.

In order to eliminate stresses in the crystal, we did a crystal annealing. The process of annealing was carried out on the plate and bulk crystal CaF_2 in the inert atmosphere of argon. The temperature of annealing of the plate was 1000 °C for 3 h, and the temperature of annealing of the bulk crystal was 1000 °C and 1080 °C for 1 - 3 h. It was noticed that after annealing, plate CaF_2 had very little stress. Annealed bulk single crystal CaF_2 had less stress than non- annealed. Upon the completion of annealing it has been observed that the crystal on the surface has a thin milky-white layer, so it is assumed that oxygen is diffused very shallow in the crystal forming CaO.

As for group theory analysis, three atoms in cubic O^5_h (Fm3m) primitive cell of the CaF_2 crystal give nine fundamental vibrations, described by the following O_h-irreducible representations (at k = 0): $\Gamma = 2T_{1u}$ (IR) + T_{2g} (Raman). According to several comprehensive work (e.g. [31-36]), their distribution among optical and acoustical are: the triply degenerate T_{2g} optical phonon is Raman active and IR inactive; one of the T_{1u} representations (triply

degenerate as well) corresponds to the zero frequency acoustic mode, while the other T_{1u} mode is actually split into a double degenerate transverse optical mode and a nondegenerate longitudinal optical mode, all the above are IR active. The room-temperature first order T_{2g} one-band Raman scattering spectrum of CaF_2 crystal is shown in Fig. 4. In this single allowed Raman optical mode with frequency ω_{SRS} = 319.7 cm^{-1} Ca^{2+} cation remains stationary and the neighboring substitutional fluoride F^{-1} ions vibrate against each other [36-39].

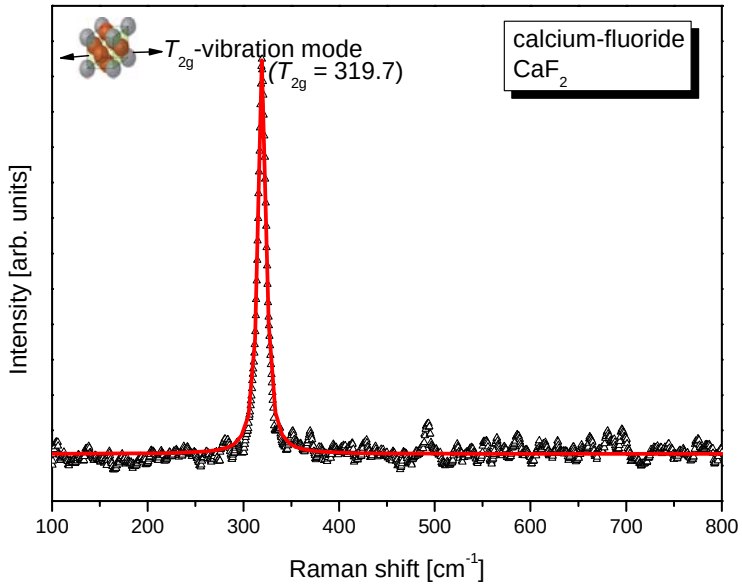

Fig. 4. Raman spectrum of CaF_2 single crystals, recorded at room temperature.

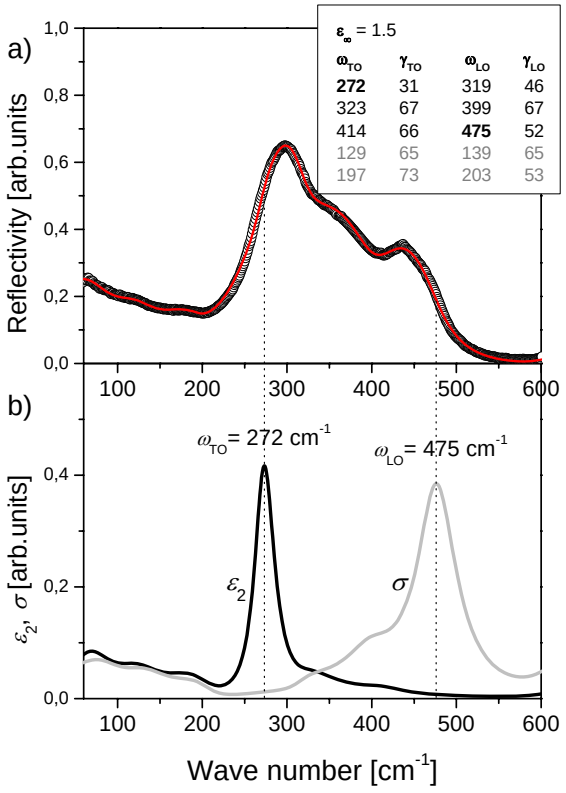

Fig. 5. IR spectrum of CaF_2 single crystals, recorded at room temperature.

The far-infrared reflectivity spectrum of the CaF_2 substrate is shown in Fig. 5. As a result of the best fit we obtained the ω_{TO} = 272 cm^{-1} and ω_{LO} = 475 cm^{-1}, little higher than in Ref. [40] (TO/LO = 257/463). In pure CaF_2, only two infrared active modes are allowed by the crystal symmetry (split TO-LO mode), but we see that the main reflectivity band of CaF_2 exhibits a feature centered about 360 cm^{-1} as a result of a two-phonon combination. This feature has been observed in all stoichiometric fluorite-structured crystals [41]. There are two additional weak modes with relatively high dampings in the range of low energies. We suppose that mode about 130 cm^{-1} could be caused by crystal impurities and about 200 cm^{-1} is a TO-mode from the X point <100>. Kramers-Kröning analysis of far-IR reflectance data gives ω_{TO} = 272 cm^{-1} and ω_{LO} = 475 cm^{-1}, in the accordance with fitting procedure (Fig. 5).

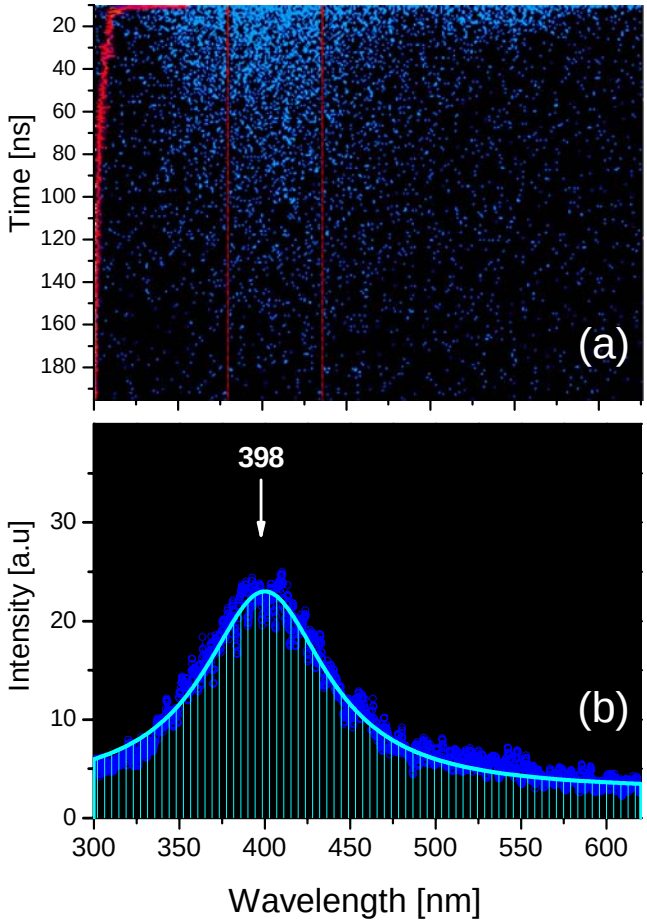

Fig. 6. Photoluminescence response of CaF_2 single crystal sample excited by 320 nm: (a) A streak camera "two-dimensional" image of the time dependent photoluminescence, (b) Fluorescence spectrum of CaF_2 crystal.

We have measured the photoluminescence response of the CaF_2 crystal sample for various excitation wavelengths and different angles of excitation beam. The streak image of the fluorescence emission spectrum of CaF_2 is presented in Fig. 6a. The photoluminescence response was very small, see Fig. 6a where typical optical response of sample is presented. Although the streak images were acquired in photon counting mode using very large number of expositions (20000), very small number of photons were counted. The vertical axis in Fig. 6a corresponds to the fluorescence development in time domain of 200 ns. The beginning of the vertical axis is cut off in order to avoid undesirable part of the spectra (excitation at 320 nm and second harmonic of Nd:YAG laser at 532 nm). Enlarged integrated profile of the

fluorescence of CaF_2 is presented in Fig. 6b. Our pure sample of CaF_2 crystal shows a broad band in 300-500 nm range. A fluorescence spectrum is obtained by averaging all events in time range from 12 ns to 190 ns after excitation. Maximum of fluorescence is on 398 nm. As pointed out in [40] this band might be induced due to the formation of color centers. These centers perhaps could be created by oxygen defects within the host of CaF_2. However, the occurrence of defects in crystal is very rare compared to the nanostructures described in [42], so the luminescence of our sample is very weak compared to the luminescence of structure described in [42]. To obtain good luminescence response, the samples of CaF_2 are doped with Ag, Eu, Tb, Cu or Dy [42, 43]. However, CaF_2 crystal is usually used in applications where high optical transmission is needed and photoluminescence is not desirable characteristics [44].

The fluorescence line profile (fluorescence decay) from image Fig. 6a is selected using the integration process in region from 340 nm to 460 nm. That profile is fitted using High Performance Digital Temporal Analyzer (HPD-TA) software, provided by Hamamatsu. The fluorescence decay is integrated in the range from 375 nm to 425 nm. Estimated lifetime of fluorescence, $\tau = 33$ ns ($\chi 2 = 1.07$), is obtained by fitting of integrated temporal profile.

The properties of the crystal, such as density of dislocations, cystallinity, and impurities concentrations, determine the optical quality.

4. Conclusions

CaF_2 single crystals in diameter of 20 mm are obtained by the vertical Bridgman method in vacuum. The crystal growth rate was 6.0 mm h^{-1}. In order to eliminate stresses in the crystal, a crystal annealing is carried out on the plate and bulk CaF_2. Number of dislocations is of the order of 5×10^4 - 2×10^5 per cm^2. The Raman T_{2g} optical mode at 319.7 cm^{-1} was observed. Kramers-Kröning analyses of the far-IR reflectance data for fluorite structure, as well as the fitting procedure, gave the same values for IR modes: $\omega_{TO} = 272$ cm^{-1} and $\omega_{LO} = 475$ cm^{-1}. Based on our work and observations during the experiment, it could be concluded that the obtained CaF_2 single crystal is of good optical quality, which was the goal of our work.

Acknowledgments

This research was financially supported by the Ministry of Education, Science and Technological Development of the Republic of Serbia through Projects No. III 45003 and TR34011.

5. References

1. D. P. Sanders, Advances in patterning materials for 193 nm immersion lithography, Chem. Rev. 110 (2010) 321-360.
2. Y. Mizumoto, T. Aoyama, Y. Kakinuma, Procedia Engineering 19 (2011) 264-269.
3. H. Ohmori, W. Lin, Y. Yamagata, S. Moriyasu, Development of Large Ultraprecision Aspheric Optics ELID Grinder for Larger X-Ray Mirrors, International Progress on Advanced Optics and Sensors, Edited by H. Ohmori and H. M. Shimizu, Universal Academy Press, Inc., Tokyo, Japan, 2003, 91-98.
4. V. Liberman, T. M. Bloomstein, M. Rothschild, J. H. C. Sedlacek, R. S. Uttaro, A. K. Bates, C. Van Peski, K. Orvek, J. Vac. Sci. Technol. B 17 (1999) 3273.
5. S. E. Swanson, American Mineralogist 62 (1977) 966-978.
6. K. Th. Wilke, J. Bohm, Crystal Growth, Harri Deutsch Press, Thun, Frankfurt/Main, 1988 (ISBN 3-87144-971-7).

7. T. Mizugaki, K. Kimura, S. Takano, US Patent 6, 123, 764 (2000).
8. T. Ohba, T. Ichizaki, US Patent 6, 270, 570 (2001).
9. G. Müller, J. Cryst. Growth 237-239 (2002) 1628-1637.
10. A. Horowitz, S. Biderman, G. B. Amer, U. Laor, M. Weiss, A. Stern, J. Cryst. Growth 85 (1987) 215-222.
11. J. T. Mouchovski, V. T. Penev, R. B. Kuneva, Cryst. Res. Technol. 31 (1996) 727-737.
12. K. A. Pandelisev, US Patent 5,993,540 (1999).
13. S. E. Gianoulakis, US Patent 6,350,310 (2002).
14. R. S. Retherford, R. Sabia, V. P. Sokira, Appl. Surf. Sci. 183 (2001) 264-269.
15. J. M. Ko, S. Tozawa, A. Yoshikawa, K. Inaba, T. Shishido, T.Oba, Y. Oyama, T. Kuwabara, T. Fukuda, J. Cryst. Growth 222 (2001) 243-248.
16. A. R. West, Solid State Chemistry and Its Applications, John Wiley&Sons, 2007.
17. P. P. Fedorov, V. V. Osiko, Bulk Crystal Growth of Electronic, Optical and Optoelectronic Materials, Edited by P. Capper, John Wiley&Sons, 2005.
18. 18. L. Su, Y. Dong, W. Yang, T. Sun, Q. Wang, J. Xu, G. Zhao, Mater. Res. Bull. 40 (2005) 619-628.
19. 19. H. Yanagi, T. Nawata, Y. Inui, Y. Hatanaka, E. Nishijima, T. Fukuda, Proc. SPIE 5377, Optical Microlithography XVII, 1886 (May 28, 2004); doi:10.1117/12.556614.
20. N. Senguttuvan, M. Aoshima, K. Sumiya, H. Ishibashi, J. Crys. Growth 280 (2005) 462-466.
21. J. Xu, M. Shi, B. Lu, X. Li, A. Wu, J. Crys. Growth 292 (2006) 391-394.
22. S. Hull, Rep. Prog. Phys. 67 (2004) 1233-1314.
23. C. Kittel, Introduction to Solid State Physics, New York, Wiley, 4th ed. 1971.
24. B. M. Voronin, S. V. Volkov, J. Phys. Chem. Solids 62 (2001) 1349-1358.
25. I. V. Stepanov, P. P. Feofilov, (1957). Artificial fluorite. In Rost kristalov (Vol. I, pp. 229), Moscow, Russia: Akademia Nauk SSSR. (in Russian).
26. D. Luković, P. M. Nikolić, S. Vujatović, S. Savić, D. Urošević, Sci. Sinter. 39 (2007) 161-167.
27. P. M. Nikolić, S. S. Vujatović, T. Ivetić, M. V. Nikolić, O. Cvetković, O. S. Aleksić, V. Blagojević, G. Brankovic, N. Nikolić, Sci. Sinter. 42 (2010) 45-50.
28. G. V. Molev, V. E. Bozhevolnov, V. I. Korobkov, V. V.Karelin, J. Crys. Growth 19 (1973) 117-121.
29. K. Recker, R. Leckebusch, J. Crys. Growth 9 (1971) 274-280.
30. H. Guggenheim, J. Appl. Phys. 34 (1963) 2482-2485.
31. R. K. Chang, B. Lacina, P. S. Pershan, Phys. Rev. Lett. 17 (1966) 755-758.
32. J. R. Ferraro, H. Horan, A. Quattrochi, J. Chem. Phys. 55 (1971) 664-666.
33. D. G. Mead, G. R. Wilkinson, J. Phys. C 10 (1977) 1063-1072.
34. D. J. Oostra, H. W. den Hartog, Phys. Rev. B 29 (1984) 2423-2432.
35. P. C. Ricci, A. Casu, G. de Giudici, P. Scardi, A. Anedda, Chem. Phys. Let. 444 (2007) 145-148.
36. A. A. Kaminskii, S. N. Bagayev, H. J. Eichler, H. Rhee, K. Ueda, K. Takaichi, K. Oka, H. Shibata, Y. Hatanaka, Y. Matsumoto, Laser Phys. Lett. 3 (2006) 385-391.
37. J. Tu, S. A. FitzGerald, J. A. Campbell, A. J. Sievers, J. Non-Cryst. Solids 203 (1996) 153-158.
38. L. Su, J. Xu, W. Yang, X. Jiang, Y. Dong, Chinese Optics Letters 3 (2005) 219-221.
39. J. P. Russell, Proceedings of the Physical Society 85 (1965) 194-196.
40. S. Ganesan, E. Burstein, Journal de Physique France 26 (1965) 645-648.

41. Kaiser, W. G. Spitzer, R. H. Kaiser, L. E. Howarth, Phys. Rev. 127 (1962) 1950-1954.
42. V. S. Singh, C. P. Joshi, S. V. Moharil, P. L. Muthalc, S. M. Dhopte, Luminescence 30 (2015) 1101-1105.
43. N. Salah, N. D. Alharbi, S. S. Habib, S. P. Lochab, J. Nanomaterials (2015) 136402, http://dx.doi.org/10.1155/2015/136402.
44. Fairfield Crystal Technology, http://www.fairfieldcrystal.com.

Садржај: *Мора се напоменути да је главни циљ овог истраживања био да се добију монокристали калцијум флуорида - CaF_2, а након тога су кристали испитивани различитим спектроскопским методама карактеризације. За раст монокристала је коришћена Брицманова метода. Под оптималним условима раста, добијени су кристали пречника до 20 mm са оријентацијом <111>. Број дислокација у кристалима CaF_2 је био 5×10^4 - 2×10^5 по cm^2. Изабрани кристал је сечен на неколико плочица дијамантском тестером. Плочице су полиране, прво силицијум карбидом, затим парафинским уљем, и на карју дијамнтском пастом. Добијени кристал је испитиван методам Раман и ИЦ спектроскопијом. Кристална структура је потврђена рендгенско структурном анализом. У складу са теоријом група примећен је један Раман и два инфрацрвена оптичка мода. Ниска фотолуминисценција сведочи о томе да је концентрација дефеката кисеоника у CaF_2 мала. Сва обављена истраживања показују да добијени монокристал CaF_2 има добар оптички квалитет, што је и био циљ овог рада.*

Кључне речи: *CaF_2, Раман спектроскопија, инфрацрвена спектроскопија, фотолуминисценција*